EXIT-Chart-Aided Hybrid Multiuser Detector for Multicarrier Interleave-Division Multiple Access

Rong Zhang, *Member, IEEE*, Lei Xu, Sheng Chen, and Lajos Hanzo, *Fellow, IEEE*

***Abstract*—A generically applicable hybrid multiuser detector (MUD) concept is proposed by appropriately activating different MUDs in consecutive turbo iterations based on the mutual information (MI) gain. It is demonstrated that the proposed hybrid MUD is capable of approaching the optimal Bayesian MUD's performance despite its reduced complexity, which is at a modestly increased complexity in comparison with that of the suboptimum soft interference cancellation (SoIC) MUD.**

***Index Terms*—EXIT charts, interleave-division multiple-access (IDMA), iterative detector.**

I. Introduction

The interleave-division multiple-access (IDMA) [1], [2] system exchanges the classic position of direct-sequence (DS) spreading and interleaving employed in traditional coded code-division multiple-access systems, leading to chip interleaving instead of bit interleaving, where users are differentiated by their unique user-specific chip interleavers. There are several advantages associated with the IDMA system. It is observed that the user-specific chip interleavers effectively enlarge the free distance of the channel code employed, and the resultant codewords of the different users constitute unique noiselike random signatures [3]. The employed chip interleaving is also capable of increasing the achievable time diversity in time-selective channels, where the burst errors are dispersed, and hence, the achievable decoding capability is improved [4]. Furthermore, IDMA is capable of striking the best tradeoff between the channel-coding rate and DS-spreading factor, hence improving the attainable error resilience [5].

Multicarrier techniques [6], [7] constitute promising enablers for employment in next-generation wireless communications and have been used, for example, in the IEEE 802.11 wireless local area network modem family and third-generation partnership project long-term evolution. A specific benefit is that upon allocating a subcarrier bandwidth, which is lower than the channel's coherent bandwidth, multicarrier techniques become capable of transforming a frequency-selective fading channel into a frequency-flat fading channel for each subcarrier. Upon concatenating a cyclic prefix (CP), the effects of the intersymbol interference (ISI) between consecutive orthogonal frequency-division multiplexing (OFDM) symbols may be avoided [8]. Thus, the further development of single-carrier IDMA to multicarrier IDMA (MC-IDMA) is beneficial when communicating over highly dispersive wideband channels. An enlightening tutorial paper about the concept of MC-IDMA can be found in [9], and the employment of the interleave-division concept to both multiplexing and multiple access was characterized in [10] and [11].

A high user load may be supported by the MC-IDMA system when employing a turbo-type iterative receiver [12], [13], where the soft information is exchanged between the multiuser detector (MUD) and channel decoder (DEC). With the advent of extrinsic information transfer (EXIT) charts [14], we are capable of analyzing, predicting, and visually comparing the convergence behaviors of different iterative receivers. Focusing on the MUD front end, the different detection algorithms have diverse EXIT characteristics, and hence, their superposition allows us to create a combined EXIT curve [11], [15], [16], which closely matches that of the DEC; hence, a near-capacity operation is facilitated.

In this paper, *we propose a novel hybrid MUD, which combines the advantages of high performance and low complexity by activating the most appropriate constituent MUD as and when it is necessary, where this activation is controlled by computing the mutual information (MI) gain in consecutive iterations based on the average value of the log-likelihood ratio (LLR) magnitudes at the output of the MUD.*

The rest of this paper is organized as follows. In Section II, we present the transceiver architecture and two typical MUD algorithms, namely, the optimum Bayesian MUD, which is also known as the maximum *a posteriori* (MAP) MUD, and the soft interference cancellation (SoIC) MUD. In Section III, we introduce the proposed hybrid MUD, while our simulation results are provided in Section IV. Finally, we conclude our discourse in Section V.

II. Transceiver Architecture

A. System Model

OFDM is capable of transforming the wideband frequency-selective channel into a set of parallel frequency-flat subcarrier channels. To elaborate a little further, instead of counteracting the effect of the frequency-selective channel $\mathbf{H}_{\mathrm{ISI}}$ by time-domain equalization, a circulant channel matrix $\mathbf{H}_c$ is constructed by concatenating the modulated signal with a CP having a length longer than the channel's memory. The circulant channel matrix $\mathbf{H}_c$ has an eigenvalue decomposition of $\mathbf{H}_c = \mathbf{U}^{\mathrm{H}}\mathbf{\Lambda}\mathbf{U}$, where $\mathbf{\Lambda}$ is a diagonal matrix hosting the eigenvalues of $\mathbf{H}_c$, and $\mathbf{U}$ is a unitary matrix, whose rows comprise the eigenvectors of $\mathbf{H}_c$. The fact that the fast Fourier transform (FFT) matrix is a unitary matrix whose rows comprise the eigenvectors of $\mathbf{H}$ by performing inverse FFT (IFFT) and FFT at the transmitter and the receiver, respectively, is often exploited. The resultant equivalent frequency-domain channel transfer function (FDCTF) is given by $\mathbf{G} = \mathbf{F}\mathbf{H}\mathbf{F}^{\mathrm{H}} = \mathbf{\Lambda}$.

The kth user's signal $\mathbf{b}_k$ is encoded by its unique user-specific channel code $\mathcal{C}_k$ at a rate of r, generating the codeword $\mathbf{x}_k = \mathcal{C}_k(\mathbf{b}_k)$. In the IDMA system, the channel code employed may be the same for all users, and a unique user-specific interleaver is employed, which defines $\mathbf{x}_k = \pi_k[\mathcal{C}(\mathbf{b}_k)]$. When a long chip interleaver is employed before the IFFT in the context of MC-IDMA, each subcarrier channel experiences more or less independent fading. Without loss of generality, we consider the mth subcarrier of the jth OFDM symbol period, where the canonical discrete-time complex baseband model of the K-user parallel OFDM communication channel seen in Fig. 1 is given by

$$y[m,j] = \sum_{k=1}^{K} h_k[m,j]x_k[m,j] + n[m,j] \tag{1}$$

where $x_k \in \{\pm 1\}$, y, and $n \sim \mathcal{CN}(0, N_0)$ denote the transmitted binary-phase-shift-keying-modulated frequency-domain signal of user k, the complex received signal, and the complex additive white Gaussian noise with variance $\sigma_n^2 = N_0/2$ per dimension, respectively. Furthermore, h_k denotes the FDCTF of user k.

Manuscript received July 24, 2009; revised October 6, 2009. First published November 17, 2009; current version published March 19, 2010. This work was supported in part by the Virtual Center of Excellence in Mobile and Personal Communications (Mobile VCE, www.mobilevce.com) under the Core 4 Research Program and in part by the Engineering and Physical Sciences Research Council. The review of this paper was coordinated by W. Zhuang.

The authors are with the School of Electronics and Computer Science, University of Southampton, SO17 1BJ Southampton, U.K. (e-mail: rz@ecs.soton.ac.uk; lh@ecs.soton.ac.uk).

Digital Object Identifier 10.1109/TVT.2009.2036874

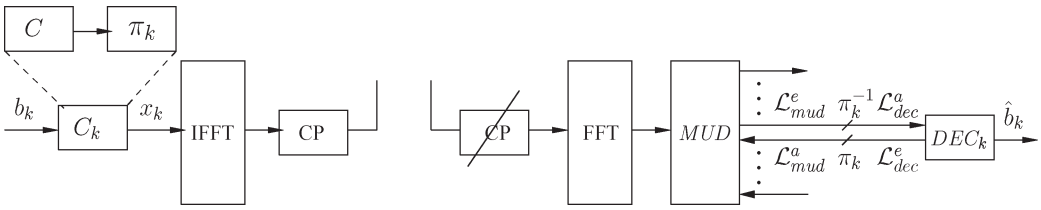

Fig. 1. Transceiver of MC-IDMA system, where the combined action of IFFT, add/removal of CP, and FFT forms a parallel OFDM channel.

B. Detection Algorithm

We employ an iterative receiver assuming perfect FDCTFs, where the long chip interleaver used facilitates the decomposition of the MUD and DEC components. Hereafter, we focus our attention on the detection algorithm and consider a single subcarrier of one OFDM symbol period, hence removing subcarrier index m and OFDM symbol index j. Furthermore, we let $\mathbf{H} = [h_1, \ldots, h_K]$ and $\mathbf{x} = [x_1, \ldots, x_K]^{\mathrm{T}}$, where the superscript $(\cdot)^{\mathrm{T}}$ denotes the transpose.

After observing the *a priori* information in terms of LLRs denoted by $\mathcal{L}^a_{\mathrm{mud}}(\mathbf{x})$, the *extrinsic* information $\mathcal{L}^e_{\mathrm{mud}}(\mathbf{x})$ is delivered by the MUD to the outer channel decoder. Based on the independence of each user's information, the *extrinsic* LLR of the kth user is given by $\mathcal{L}^e_{\mathrm{mud}}(x_k) = \mathcal{L}_{\mathrm{mud}}(x_k) - \mathcal{L}^a_{\mathrm{mud}}(x_k)$.

1) Optimum Bayesian Detection: Let us first discuss the *extrinsic* information $\mathcal{L}^e_{\mathrm{mud}}(x_k)$ delivered by the optimum Bayesian MUD, which is calculated as

$$\mathcal{L}^e_{\mathrm{mud}}(x_k) = \ln \frac{p(y|x_k = +1, \mathbf{x}_{-k})}{p(y|x_k = -1, \mathbf{x}_{-k})} \tag{2}$$

where $\mathbf{x}_{-k}$ denotes the vector $\mathbf{x}$ having its kth entry excluded. The conditional probability density function (pdf) $p(y|x_k = \pm 1, \mathbf{x}_{-k})$ can be computed by subtracting the *a priori* probability $P(x_k = \pm 1)$ of the particular symbol from the joint pdf $p(y, x_k = \pm 1, \mathbf{x}_{-k})$

$$\begin{aligned} p(y|x_k = \pm 1, \mathbf{x}_{-k}) &= \frac{p(y, x_k = \pm 1, \mathbf{x}_{-k})}{P(x_k = \pm 1)} \\ &= \sum_{\mathbf{x}: x_k = \pm 1} \frac{p(y|\mathbf{x}) P(\mathbf{x})}{P(x_k = \pm 1)} \\ &= \sum_{\mathbf{x}: x_k = \pm 1} p(y|\mathbf{x}) \prod_{i \neq k} P(x_i) \end{aligned} \tag{3}$$

where the last equation holds when each user's information is independent. The *a priori* probability $P(x_i)$ can be obtained from the LLR $L^e_{\mathrm{dec}}(x_i)$ fed back to the MUD by the DEC after interleaving, which can be expressed as [13]

$$\begin{aligned} P(x_i = \pm 1) &= \frac{\exp[\pm \mathcal{L}^e_{\mathrm{dec}}(x_i)]}{1 + \exp[\pm \mathcal{L}^e_{\mathrm{dec}}(x_i)]} \\ &= \frac{\exp[\pm \mathcal{L}^e_{\mathrm{dec}}(x_i)/2]}{\exp[\mp \mathcal{L}^e_{\mathrm{dec}}(x_i)/2] + \exp[\pm \mathcal{L}^e_{\mathrm{dec}}(x_i)/2]} \\ &= \cosh\left[\mathcal{L}^e_{\mathrm{dec}}(x_i)/2\right] \frac{1 \pm \tanh\left[\mathcal{L}^e_{\mathrm{dec}}(x_i)/2\right]}{2\cosh\left[\mathcal{L}^e_{\mathrm{dec}}(x_i)/2\right]} \\ &= \frac{1}{2} \pm \frac{1}{2} \tanh\left[\mathcal{L}^e_{\mathrm{dec}}(x_i)/2\right]. \end{aligned} \tag{4}$$

On the other hand, the conditional likelihood function $p(y|\mathbf{x})$ may be expressed as

$$p(y|\mathbf{x}) \propto \exp\left(-\frac{\|y - \mathbf{H}\mathbf{x}\|^2}{2\sigma_n^2}\right) \tag{5}$$

where $\propto$ represents "proportional to." Thus, the extrinsic information $\mathcal{L}^e_{\mathrm{mud}}(x_k)$ is given by

$$\begin{aligned} \mathcal{L}^e_{\mathrm{mud}}(x_k) &= \ln \frac{p(y|x_k = +1, \mathbf{x}_{-k})}{p(y|x_k = -1, \mathbf{x}_{-k})} \\ &= \ln \frac{\sum_{\mathbf{x}: x_k = +1} \exp(-\|y - \mathbf{H}\mathbf{x}\|^2/2\sigma_n^2)\, \phi}{\sum_{\mathbf{x}: x_k = -1} \exp(-\|y - \mathbf{H}\mathbf{x}\|^2/2\sigma_n^2)\, \phi} \end{aligned} \tag{6}$$

where $\phi = \prod_{i \neq k} P(x_i)$, and $P(x_i)$ is given by (4). The extrinsic information $\mathcal{L}^e_{\mathrm{mud}}(x_k)$ is then deinterleaved and fed to the DEC in Fig. 1.

2) SoIC: The optimum Bayesian detection exhibits a prohibitive complexity; thus, as a design alternative, we also introduce a reduced-complexity SoIC-type MUD. Let us rewrite (1) as

$$y = h_k x_k + \xi \tag{7}$$

where ξ denotes the interference plus noise formulated as $\xi = \sum_{i \neq k} h_i x_i + n$. By approximating ξ as a joint Gaussian random variable, which can be justified by the central limit theorem provided that the number of users K supported is sufficiently high, we have the *extrinsic* information as [1]

$$\begin{aligned} \mathcal{L}^e_{\mathrm{mud}}(x_k) &= \ln \frac{p(y|x_k = +1)}{p(y|x_k = -1)} \\ &= \ln \frac{\exp\left(\|y - \hat{\xi} - h_k\|^2/2\mathbf{R}_\xi\right)}{\exp\left(\|y - \hat{\xi} + h_k\|^2/2\mathbf{R}_\xi\right)} \\ &= 2h_k^* \mathbf{R}_\xi^{-1} (y - \hat{\xi}) \end{aligned} \tag{8}$$

where the superscript $(\cdot)^*$ denotes conjugate, and $\hat{\xi} = \sum_{i \neq k} h_i \hat{x}_i$ denotes an estimate of the parameter ξ, while $\mathbf{R}_\xi$ represents the variance of the interference plus noise, which is formulated as

$$\begin{aligned} \mathbf{R}_\xi &= \mathbf{R}_y - v_k h_k h_k^* \\ &= \mathbf{H}\mathbf{V}\mathbf{H}^{\mathrm{H}} + \sigma_n^2 \mathbf{I} - v_k h_k h_{k,u}^* \end{aligned} \tag{9}$$

where the instantaneous variance v_i, which is the ith diagonal entry of $\mathbf{V} = \mathrm{diag}[v_1, \ldots, v_K]$, and the soft estimate $\hat{x}_i$ are given by

$$\begin{aligned} \hat{x}_i &= \sum_{\alpha \in \pm 1} \alpha P(\hat{x}_i = \alpha) \\ &= \tanh\left[\frac{\mathcal{L}^e_{\mathrm{dec}}(x_i)}{2}\right] \end{aligned} \tag{10}$$

$$\begin{aligned} v_i &= E\left(\hat{x}_i^2\right) - E(\hat{x}_i)^2 \\ &= 1 - \hat{x}_i^2. \end{aligned} \tag{11}$$

Remarks: It can be seen in the aforementioned derivation that only the knowledge of $\hat{x}_i$ is needed for the *extrinsic* information $\mathcal{L}^e_{\mathrm{mud}}(x_k)$ for the SoIC MUD. Instead of the exponential complexity of the Bayesian MUD as a function of the number of users K, the

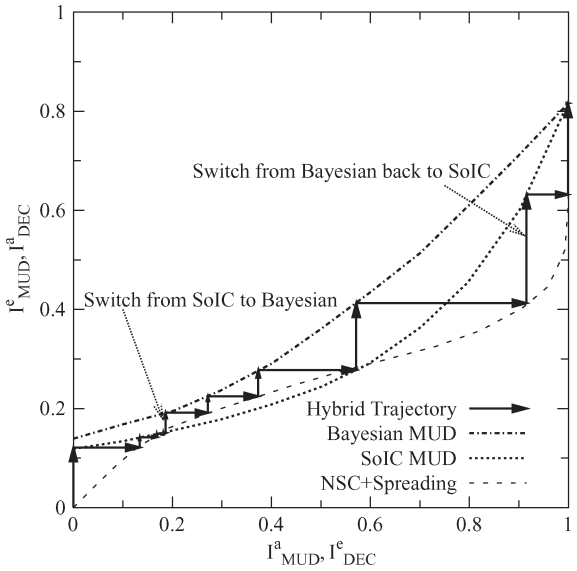

Fig. 2. EXIT charts and simulated trajectories of the proposed hybrid MUD when supporting $K = 12$ users at $E_b/N_0 = 10$ dB.

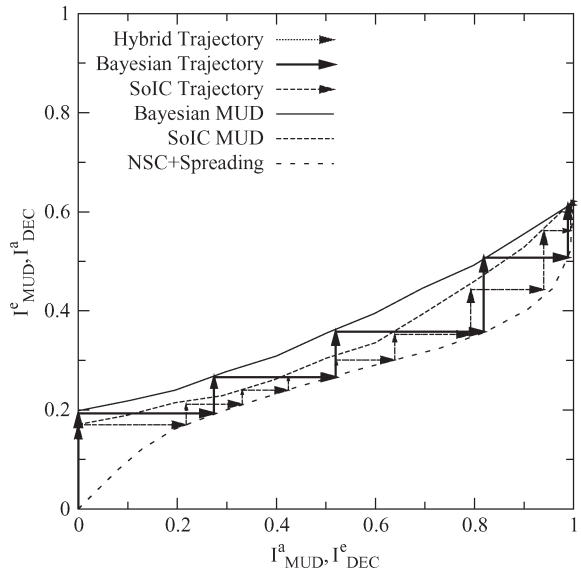

Fig. 3. EXIT charts and simulated trajectories of the proposed hybrid MUD when supporting $K = 8$ users at $E_b/N_0 = 6$ dB.

low-complexity SoIC-aided MUD has a linearly increasing complexity as a function of K.

III. Hybrid Detector Design

A. EXIT Chart Analysis

EXIT charts, which are widely used in the analysis of turbo-type iterative systems, were introduced by ten Brink [14]. This technique relies on computing the MI of the constituent soft components. It evaluates the nonlinear function $I^e = \chi(I^a)$, which maps the input *a priori* MI $I^a \in [0, 1]$ to the output *extrinsic* MI $I^e \in [0, 1]$, where the amount of the output *extrinsic* MI I^e gleaned from the input *a priori* MI I^e determines the convergence behavior of this soft component. Since the *extrinsic* information generated by the first component acts as the *a priori* information for the second component and *vice versa*, in the EXIT charts, we alternately swap the abscissa and ordinate axes, depending on which of the two components acts as the source of *a priori* information, corresponding to the abscissa.

Fig. 2 portrays the EXIT curves of both the SoIC MUD and the Bayesian MUD when supporting $K = 12$ users with the aid of the combination of a rate-1/2 nonsystematic convolutional (NSC) code and two-chip DS-spreading sequences at $E_b/N_0 = 10$ dB over a three-path short wireless asynchronous transfer mode (SWATM) channel [6], where the number of subcarriers and the length of CP were set to 128 and 32, respectively. On the left side of Fig. 2, which corresponds to the *interference-limited* region [11], the Bayesian MUD outputs only marginally higher *extrinsic* information than the SoIC MUD. As the amount of available *a priori* information increases, the discrepancy between these two EXIT curves becomes more substantial, owing to the suboptimal nature of the SoIC MUD, albeit this is achieved at the cost of tremendously increased computational complexity by the Bayesian MUD. Ultimately, these two curves tend to the corresponding single-user performance when the effects of interference have been more or less eliminated, corresponding to the *noise-limited* region [11] on the right side of Fig. 2. This leads to the complexity-versus-performance tradeoff.

When there may not be a sufficiently widely open convergence tunnel for the SoIC MUD, but it may still be open for the Bayesian MUD, as seen in Fig. 2, our novel proposition is to use the SoIC MUD during the first few iterations and to subsequently activate the Bayesian MUD for a few further iterations to avoid encountering the "bottleneck" region of the SoIC MUD, beyond which, we may then safely again activate the SoIC MUD. As seen in Fig. 2, the simulation-based hybrid MUD's trajectory closely follows the EXIT curves of the receiver components. As an explicit benefit, the proposed hybrid MUD becomes capable of performing similarly to that of the Bayesian MUD at a decreased complexity, since the Bayesian MUD is only activated during the critical iterations.

Fig. 3 shows both the EXIT curves and the associated simulation-based trajectories of all the MUDs concerned when supporting $K = 8$ users at $E_b/N_0 = 6$ dB. At this particular E_b/N_0 value, there is no need to activate the Bayesian MUD, since even the lower complexity SoIC MUD is capable of maintaining an open EXIT tunnel, hence lending to an infinitesimally low bit-error ratio (BER).

B. MI Gain

For the sake of determining the activation instant of the different MUDs, we have to monitor the MI gain of the MUDs between the consecutive iterations at the receiver. In practice, the MI is generally unknown at the receiver, and there is a difference between the EXIT-chart-based MI prediction and the practical decoding trajectory. Thus, we have to contrive a realistic measure of the MI gain used to control the activation of the constituent MUDs. This can be achieved by estimating the *extrinsic* LLRs' average magnitude $E(|\mathcal{L}^e_{\rm mud}|)$ at the output of the MUD.

Provided that a long interleaver is employed, the pdf of the *extrinsic* LLRs' magnitude may be assumed to obey

$$p\left(|\mathcal{L}^e_{\rm mud}|\right) = \frac{2}{\sigma_{\rm LLR}\sqrt{2\pi}} \exp\left(-\frac{|\mathcal{L}^e_{\rm mud}|^2}{2\sigma^2_{\rm LLR}}\right) \tag{12}$$

where $\sigma_{\rm LLR}$ is the variance of LLRs. Hence, we have

$$E\left(|\mathcal{L}^e_{\rm mud}|\right) = \int_0^{+\infty} \frac{2x}{\sigma_{\rm LLR}\sqrt{2\pi}} \exp\left(-\frac{x^2}{2\sigma^2_{\rm LLR}}\right) dx$$

$$= \sqrt{\frac{2}{\pi}}\sigma_{\rm LLR}. \tag{13}$$

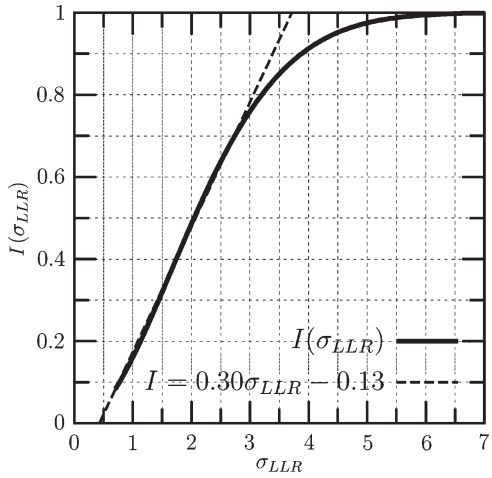

Fig. 4. MI I function of $\sigma_{\rm LLR}$ and its linear approximation.

The MI was shown to be a monotonically increasing J-function of the variance of LLRs [14], i.e., $I(\sigma_{\rm LLR}) = J(\sigma_{\rm LLR})$. By taking into account (13) and letting the *extrinsic* LLRs' average magnitude $\epsilon = E(|\mathcal{L}^e_{\rm mud}|)$, we arrive at $I(\epsilon) = J(\epsilon\sqrt{\pi/2})$, where the J-function can be closely approximated by

$$J(x) \approx (1 - 2^{-H_1 x^{2H_2}})^{H_3} \tag{14}$$

where we have $H_1 = 0.3073$, $H_2 = 0.8935$, and $H_3 = 1.1064$. The resultant function is straightforward polynomial fitting, which is not detailed here.

Since the MI range of $I \in [0.1, 0.8]$ typically covers the "bottleneck" region of the EXIT tunnel during the iterative process, in this range, the more powerful Bayesian MUD is activated in our hybrid MUD approach. We can use a first-order linear function to approximate the nonlinear J-function in the range of [0.1,0.8], as seen in Fig. 4, where the MI associated with the Gaussian assumption can be accurately approximated by $I(\sigma_{\rm LLR}) \approx 0.3043\sigma_{\rm LLR} - 0.1303$. Subsequently, by taking into account (13), we arrive at

$$I(\epsilon) \approx 0.3043\sqrt{\frac{\pi}{2}}\epsilon - 0.1303. \tag{15}$$

Hence, we can contrive a realistic low-complexity linear scheme[1] of estimating the *extrinsic* MI at the output of the MUD based on (15). For the sake of activating the appropriate constituent MUD in our hybrid MUD scheme, we record the *extrinsic* LLRs' average absolute value ϵ and arrive at the *extrinsic* MI gain of consecutive iterations

$$G(q) = I^{e,q}_{\rm mud} - I^{e,q-1}_{\rm mud} \tag{16}$$

where q denotes iteration index.

C. Algorithmic Summary

More explicitly, the detailed steps of our novel hybrid MUD scheme are listed as follows, and all the parameters ρ_1, ρ_2, ρ_3 are experimentally obtained.

1) Initially, we activate the SoIC MUD.
2) Once we encounter $G(q) < \rho_1 = 0.05$ and, simultaneously, $I^{e,q}_{\rm mud} < \rho_2 = 0.6$, the more complex but more powerful Bayesian MUD is activated. This allows the MUD to traverse through the "bottleneck" region of $I^e_{\rm mud} \in [0.1, 0.3]$ seen in Fig. 2.

[1]Our goal was to use an approximation employing a low-complexity linear polynomial, although the approximation mentioned in [17] is also applicable.

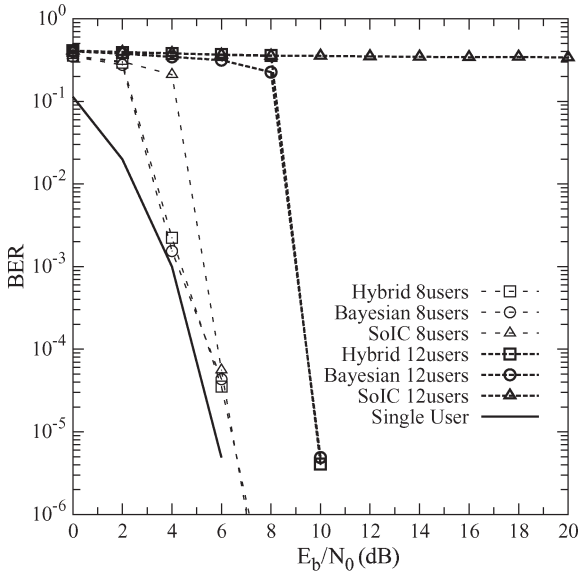

Fig. 5. BER performance of the proposed system.

3) When we encounter $G(q) > \rho_3 = 0.12$, the low-complexity SoIC MUD is reactivated for the sake of reducing the overall complexity.
4) A sufficiently high $G(q)$ should always be maintained after switching to the SoIC MUD. As and when this condition is not satisfied, the Bayesian MUD should be reactivated.

In other words, the proposed hybrid MUD will always activate the low-complexity SoIC MUD as and when the EXIT curve of the SoIC MUD is sufficiently higher than that of the DEC, while the Bayesian MUD will be employed in the rest of the cases.

IV. Simulation Results

A. Performance

We now investigate the attainable performance of the proposed hybrid MUD, in comparison with the two constituent MUDs. We employ a rate-1/2 convolutional code in conjunction with a rate-1/2 NSC code, resulting in an overall code rate of $r = 1/4$. An information packet length was set to 1024, and a three-path SWATM channel was considered, where the number of subcarriers and the length of CP were set to 128 and 32, respectively. Fig. 5 portrays the attainable BER performance of the SoIC MUD, the Bayesian MUD, and the proposed hybrid MUD as a function of both E_b/N_0 and the number of users K. Observe in Fig. 5 that, at a high normalized user load of $\beta = Kr = 12/4 = 3$, the SoIC MUD fails to converge, while the proposed hybrid MUD and the Bayesian MUD achieves an infinitesimally low BER for $E_b/N_0 > 10$ dB.

B. Complexity

The complexity of the hybrid MUD is determined by the complexity of the SoIC MUD and that of the Bayesian MUD, weighted by the corresponding number of iterations, i.e.,

$$\mathcal{O} = Q_{\rm SoIC}\mathcal{O}(K) + Q_{\rm Bay}\mathcal{O}(2^K). \tag{17}$$

Compared with the stand-alone Bayesian MUD, the proposed hybrid MUD achieves a significant complexity reduction. This is because, in our hybrid MUD, the Bayesian MUD is only activated during a few critical iterations, while the remaining SoIC iterations impose only

a small complexity. More explicitly, in Fig. 2, there are $Q_{\mathrm{SoIC}} = 5$ iterations and $Q_{\mathrm{Bay}} = 4$ iterations, while the stand-alone Bayesian MUD requires $Q_{\mathrm{Bay}} = 7$ iterations, which approximately halves the complexity imposed. This is not shown in Fig. 2, since the trajectory of the stand-alone Bayesian MUD would obfuscate that of the hybrid MUD.

V. Conclusion

In this paper, we have proposed a novel hybrid MUD scheme by switching between different MUDs based on the MI gain. Our scheme combines the benefits of both low complexity and high performance and strikes an attractive tradeoff between the constituent MUDs employed as benchmarkers. Simulation results quantified the performance advantage of employing the hybrid MUD: At normalized user load of $\beta = 3$, the SoIC MUD failed to converge, whereas the proposed hybrid MUD achieved an infinitesimally low BER, which was similar to that of the optimal Bayesian MUD, while imposing only about half the complexity.

Acknowledgment

Fully detailed technical reports on this work are available to Industrial Members of Mobile VCE.

References

[1] P. Li, L. H. Liu, K. Y. Wu, and W. K. Leung, "Interleave-division multiple-access," *IEEE Trans. Wireless Commun.*, vol. 5, no. 4, pp. 938–947, Apr. 2006.

[2] H. Schoeneich and P. A. Hoeher, "Adaptive interleave-division multiple access—A potential air interference for 4G bearer services and wireless LANs," in *Proc. WOCN*, Muscat, Oman, Jun. 7–9, 2004, pp. 179–182.

[3] P. Frenger, P. Orten, and T. Ottosson, "Code-spread CDMA using maximum free distance low-rate convolutional codes," *IEEE Trans. Wireless Commun.*, vol. 48, no. 1, pp. 135–144, Jan. 2000.

[4] D. Gargy and F. Adachi, "Comprehensive evaluation of chip interleaving effect on turbo-coded DS-SS in a Rayleigh fading channel with antenna diversity reception," *Wireless Commun. Mobile Comput.*, vol. 6, no. 1, pp. 49–60, Feb. 2006.

[5] R. Zhang and L. Hanzo, "EXIT chart based joint code-rate and spreading-factor optimisation of single-carrier interleave division multiple access," in *Proc. IEEE WCNC*, Hong Kong, Mar. 11–15, 2007, pp. 735–739.

[6] L. Hanzo, M. Munster, B. J. Choi, and T. Keller, *OFDM and MC-CDMA for Broadcasting Multi-User Communications, WLANs and Broadcasting*. New York: Wiley-IEEE Press, 2003.

[7] L. Hanzo, L. L. Yang, E. L. Kuan, and K. Yen, *Single- and Multi-Carrier DS-CDMA: Multi-User Detection, Space-Time Spreading, Synchronisation, Networking and Standards*. New York: Wiley-IEEE Press, 2003.

[8] A. J. Goldsmith, *Wireless Communication*. Cambridge, U.K.: Cambridge Univ. Press, 2005.

[9] P. Li, Q. H. Guo, and J. Tong, "The OFDM-IDMA approach to wireless communication systems," *IEEE Wireless Commun.*, vol. 14, no. 3, pp. 18–24, Jun. 2007.

[10] P. Hoeher and W. Xu, "Multi-layer interleave-division multiple access for 3GPP long term evolution," in *Proc. ICC*, Glasgow, U.K., Jun. 24–28, 2007, pp. 5508–5513.

[11] R. Zhang and L. Hanzo, "Three design aspects of multicarrier interleave division multiple access," *IEEE Trans. Veh. Technol.*, vol. 57, no. 6, pp. 3607–3617, Nov. 2008.

[12] L. Hanzo, T. H. Liew, and B. L. Yeap, *Turbo Coding, Turbo Equalisation and Space-Time Coding for Transmission Over Fading Channels*. New York: Wiley-IEEE Press, 2002.

[13] X. D. Wang and H. V. Poor, "Iterative (turbo) soft interference cancellation and decoding for coded CDMA," *IEEE Trans. Commun.*, vol. 47, no. 7, pp. 1046–1061, Jul. 1999.

[14] S. ten Brink, "Convergence behavior of iteratively decoded parallel concatenated codes," *IEEE Trans. Commun.*, vol. 49, no. 10, pp. 1727–1737, Oct. 2001.

[15] L. Hanzo, O. Alamri, M. El-Hajjar, and N. Wu, *Near-Capacity Multi-Functional MIMO Systems: Sphere Packing Modulation, Iterative Detection and Cooperation*. New York: Wiley-IEEE Press, Apr. 2009.

[16] R. Zhang, L. Xu, S. Chen, and L. Hanzo, "Repeat accumulate code division multiple access and its hybrid detection," in *Proc. IEEE ICC*, Beijing, China, May 19–23, 2008, pp. 4790–4794.

[17] J. Hagenauer, "The turbo principle in mobile communications," in *Proc. Nordic Radio Symp.*, Oulu, Finland, Aug. 16–18, 2004.

Exploring the Dynamic Nature of Mobile Nodes for Predicting Route Lifetime in Mobile Ad Hoc Networks

Xin Ming Zhang, Feng Fu Zou, En Bo Wang, and Dan Keun Sung

***Abstract*—In mobile ad hoc networks, a host may exhaust its power or move away without giving any notice to its cooperative nodes, causing changes in network topology, and thus, these changes may significantly degrade the performance of a routing protocol. Several routing protocol studies based on node lifetime and link lifetime have been done to address this problem. We propose a new algorithm to evaluate the node lifetime and the link lifetime utilizing the dynamic nature, such as the energy drain rate and the relative mobility estimation rate of nodes. Integrating these two performance metrics by using the proposed route lifetime-prediction algorithm, we select the least dynamic route with the longest lifetime for persistent data forwarding. Finally, we implement our proposed route lifetime-prediction algorithm in an exploring dynamic nature routing (EDNR) protocol environment based on dynamic source routing (DSR) and compare the performance through simulations. The EDNR protocol outperforms the conventional DSR protocols that are implemented with lifetime-prediction routing (LPR) and signal-stability-based adaptive (SSA) routing mechanisms.**

***Index Terms*—Lifetime prediction, link lifetime (LLT), mobile ad hoc networks (MANETs), node lifetime, route discovery, routing protocol.**

I. Introduction

A mobile ad hoc network (MANET) consists of many mobile nodes that can communicate with each other directly or through intermediate nodes. Often, hosts in a MANET operate with batteries and can roam freely, and thus, a host may exhaust its power or move away, giving no notice to its neighboring nodes, causing changes in network topology. One of the important and challenging problems in the design of ad hoc networks is the development of an efficient routing protocol that can provide high-quality communications among mobile hosts. Several studies on the dynamic nature of MANETs have been done. These studies often attempt to find a stable route that has a long lifetime [1]. We can classify these solutions into two main groups: node lifetime routing algorithms and link lifetime (LLT) routing algorithms.

By considering the energy state of nodes, such as residual energy and energy drain rate, the node lifetime routing algorithms often select

Manuscript received July 27, 2009; revised October 13, 2009. First published December 18, 2009; current version published March 19, 2010. This work was supported in part by the National Natural Science Foundation of China under Grant 60673171 and in part by the National Grand Fundamental Research 973 Program of China under Grant 2006CB303006. The review of this paper was coordinated by Prof. J. Misic.

X. M. Zhang, F. F. Zou, and E. B. Wang are with the School of Computer Science and Technology, University of Science and Technology of China, Hefei 230027, China (e-mail: xinming@ustc.edu.cn; fengfu@mail.ustc.edu.cn; wangeb@mail.ustc.edu.cn).

D. K. Sung is with the Korea Advanced Institute of Science and Technology, Daejeon 305-701, Korea (e-mail: dksung@ee.kaist.ac.kr).

Digital Object Identifier 10.1109/TVT.2009.2038708